Effective potential energies and transport cross sections for atom-molecule interactions of nitrogen and oxygen

James R. Stallcop and Harry Partridge
NASA Ames Research Center, Moffett Field, California 94035-1000

Eugene Levin
Eloret Corporation, Moffett Field, California 94035-1000

(Received 15 June 2001; published 19 September 2001)

The potential energy surfaces for H_2-N and N_2-N interactions are calculated by accurate *ab initio* methods and applied to determine transport data. The results confirm that an effective potential energy for accurately determining transport properties can be calculated using a single predetermined orientation. A simple method is developed to determine the dispersion coefficients of effective potential energies. Effective potential energies required for O_2-O collisions are determined. The H_2-N, N_2-N, O_2-H, and O_2-O collision integrals are calculated and tabulated for a broad range of temperatures. The theoretical values of the N_2-N and O_2-O diffusion coefficients compare well with measured data available at room temperature.

DOI: 10.1103/PhysRevA.64.042722 PACS number(s): 34.20.Cf, 31.15.Dv, 51.20.+d

I. INTRODUCTION

The transport properties of the interactions of hydrogen, nitrogen, and oxygen are required for studies of certain hydrogen-burning propulsion systems [1] and the environment [2–4] of space vehicles. Atom-molecule transport coefficients are needed for the study [5–7] of certain physical and chemical processes. For example, the diffusion coefficients of oxygen and nitrogen have been used for the analysis of etching [8] and deposition [9] processes and the measurement [10] of the rates of chemical reactions.

The atom-molecule diffusion coefficients of nitrogen and oxygen have been measured [11] at room temperature and can be determined at high temperatures from interaction energies that have been deduced [2,12–14] from high-energy scattering experiments. Measurements for a small range of energies or temperatures alone, however, are not sufficient [15] to allow the determination of a unique interaction energy for the prediction of reliable transport properties outside the range of the experimental energies or temperatures.

The calculation of potential energies required for conventional determinations of transport properties can be a very laborious task, especially, when a number of states of the system are needed to describe the scattering process. Moreover, these calculations become impractical for systems involving the interactions of large molecules, such as those required for studying or modeling the deposition and etching processes for the preparation [16] of certain electronic devices. To overcome this problem, we have applied [15] molecular symmetry to identify effective potential energies that reduce the computational effort by a large factor and still yield accurate approximations to those transport properties such as diffusion and viscosity that are dominated by elastic scattering processes. Physically realistic effective potential energies are important for the correlation [17] of measured data or the prediction of the transport properties of more complex interactions using the Aufbau method [15] to obtain the short-range interaction energy.

In the present work, we extend our atom-molecule studies by determining the effective potential energies and the transport properties of the interactions of chemically active collision partners, which are very difficult to measure in the laboratory.

The atom-molecule interaction energies are described in Sec. II. An Aufbau method for readily estimating the long-range coefficients of effective potential energies is described in the Appendix. The application of the interaction energies to transport data is contained in Sec. III. Conclusions are summarized in Sec. IV.

II. ATOM-MOLECULE INTERACTION ENERGIES

A. Atom-molecule interactions

The geometry for atom–homonuclear-molecule orientations is specified in terms of the separation distance r from the atom to the center of mass of the homonuclear diatomic molecule, and the angle θ between a line joining the atom with the center of mass of the molecule and the molecular symmetry axis passing through the nuclear centers.

Properties $F(x,\theta)$, such as the interaction energy $V(r,\theta)$ or scattering cross sections [15] $Q(E,\theta)$ for collision energy E, that are governed by the symmetry of an atom–diatomic-molecule can be represented by expansions in Legendre polynomials $P_n(\cos\theta)$. For homonuclear molecules, the expansion can be expressed in the form

$$F(x,\theta)=\sum_{n=0} F_{2n}(x)P_{2n}(\cos\theta). \tag{1}$$

For interactions involving hydrogen or rare-gas atoms that have small anisotropy, the spherically averaged potential $\overline{V}(r)$, which can be obtained from the leading term on the right-hand side (RHS) of Eq. (1), can be approximated well [15,18,19] by $V(r,\theta_0)$ at large r where the angle θ_0 satisfies

$$P_2(\cos\theta_0)=0; \tag{2}$$

i.e., $\theta_0=54.735\,610\,3°$. Even though the angular variation in $V(r,\theta)$ may be large, transport cross sections tend to have a

much smaller variation with respect to θ. From the sudden scattering approximations described below, it follows that $V(r,\theta_0)$ can be considered an effective potential energy for the approximate determination of transport cross sections.

B. H_2-N and N_2-N potential-energy surfaces

The H_2-N and N_2-N rigid-rotor potential-energy surfaces are calculated using high-level quantum chemistry methods. Specifically, a restricted coupled-cluster singles and doubles approach [20,21] that includes a perturbational correction [22,23] for triples [RCCSD(T)] is combined with large basis sets; the atom-centered basis sets are obtained from the augmented correlation-consistent polarized-valence quadruple zeta (AQZ) of Dunning and co-workers [24–26]. In addition, for N_2-N, we add [15] bond functions to the basis sets and use the counterpoise method [27] to remove basis set superposition error (BSSE). Partridge and Bauschlicher [28] have examined convergence for weak molecular binding; reliable values of the potential energy can be obtained with the bond-function approach outlined above.

The values of $V(r,\theta)$ are calculated for a broad range of r at the θ values 0°, 30°, 45°, θ_0, 60°, and 90°. The H_2-N calculation also includes values for the angle 10°; in addition, some values at 80° and small r were determined to test the accuracy of the values predicted by an analytic potential-energy fit to the data for the other seven angles. For N_2-N, the BSSE corrections for $V(r,\theta)$ at 45° and 60° were obtained from the corrections from the other angles using a procedure [29] for adding improvements from larger basis sets to certain calculated energies. Some of our calculated results for H_2-N and N_2-N are shown in Figs. 1 and 2, respectively, for large r. Note that the curves for $V(r,\theta_0)$ and $\overline{V}(r)$ of NH_2, which has small anisotropy, are nearly indistinguishable.

The calculated data for $V(r,\theta)$ at large r can be fitted fairly well by a modified Tang-Toennies potential-energy function $V_{MTT}(r,\theta)$. A general formulation of V_{MTT} for molecular interactions is described in Ref. [15]; a simplified form for atom-molecule interactions is listed here for convenience. For homonuclear molecules, this potential-energy function is expressed by the sum

$$V_{MTT}(r,\theta)=V_{SR}(r,\theta)+V_{DLR}(r,\theta) \tag{3a}$$

where the short-range repulsive exchange energy V_{SR} and the damped long-range attractive energy V_{DLR} have the forms

$$\ln V_{SR}(r,\theta)=a(\theta)-\alpha(\theta)r, \tag{3b}$$

$$V_{DLR}(r,\theta)=-\sum f_{2n}[\alpha(\theta)r]\frac{C_{2n}(\theta)}{r^{2n}}. \tag{3c}$$

The quantities a and α^{-1} characterize the strength and range, respectively, of the repulsive energy. The quantities $C_{2n}(\theta)$ are the coefficients of the long-range forces and the damping function f_{2n} is obtained [15] from an incomplete γ function.

The coefficients of quantities $a(\theta)$, $\alpha(\theta)$, and $C_{2n}(\theta)$ for the expansions in $P_{2n}(\cos\theta)$ specified by Eq. (1) are listed in Table I for both H_2-N and N_2-N interactions. The determination of leading terms of the higher-order values of C_{2n} is described in the Appendix. The $a(\theta)$ and $\alpha(\theta)$ for determining the values of Table I are obtained using the iterative procedure that is described in Ref. [15] and a least-squares fit to the calculated data for $r \geqslant 4.5a_0$ and $r \geqslant 5.5a_0$ for H_2-N and N_2-N, respectively.

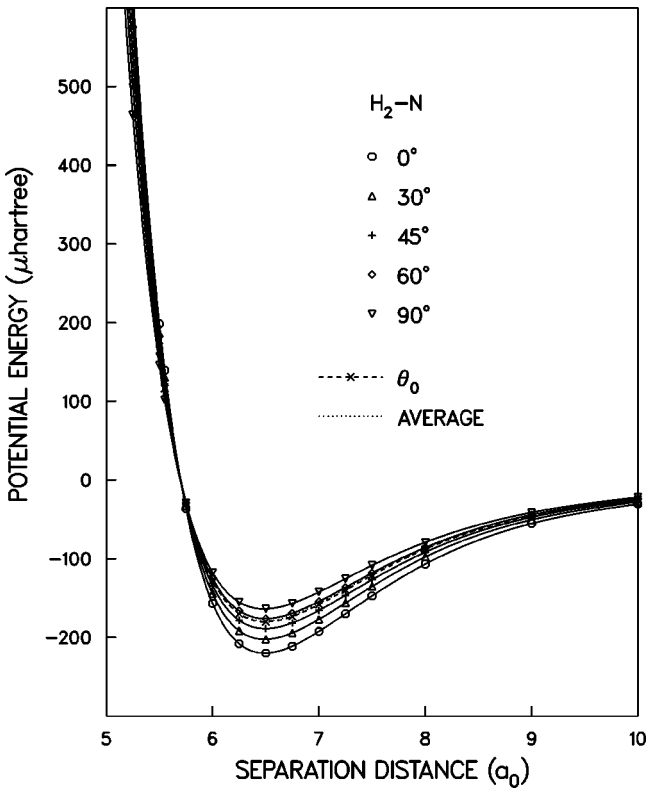

FIG. 1. H_2-N potential-energy curves at large r. The data points represent the calculated results of the present work and the curves are determined from spline fits to the data.

For applications such as scattering calculations that require higher accuracy for V at smaller r where the interaction is not dominated by the long-range forces, we construct a fit using the polynomial expansion of Eq. (1). We have shown [15,33] that this can be accomplished very efficiently with $\ln[V_{SR}(r,\theta)]$; the uniform behavior of $\ln[V_{SR}(r,\theta)]$ allows a significant reduction in the number of data points required for an accurate fit.

The values of the short-range energy

$$V^c_{SR}(r,\theta)=V^c(r,\theta)-V_{DLR}(r,\theta), \tag{4}$$

where $V^c(r,\theta)$ represents the computed values and $V_{DLR}(r,\theta)$ is calculated using Eq. (3c) and the values of the parameters from Table I, are shown in Figs. 3 and 4 for H_2-N and N_2-N, respectively. Note that the near-uniform splitting of the solid curves shown in Figs. 3 and 4 indicates that the angular variation in $\ln[V^c_{SR}(r,\theta)]$ is described primarily by $P_2(\cos\theta)$.

The coefficients of $\ln[V^c_{SR}(r,\theta)]$ for the expansion in $P_{2n}(\cos\theta)$ of Eq. 1 are determined from a least-squares fit

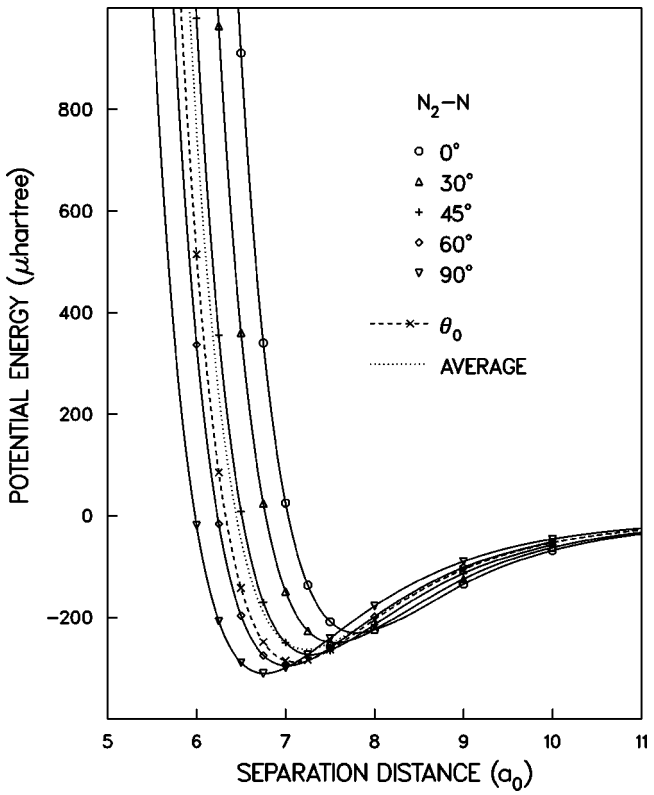

FIG. 2. N_2-N potential-energy curves at large r. The data points represent the calculated results of the present work and the curves are determined from spline fits to the data.

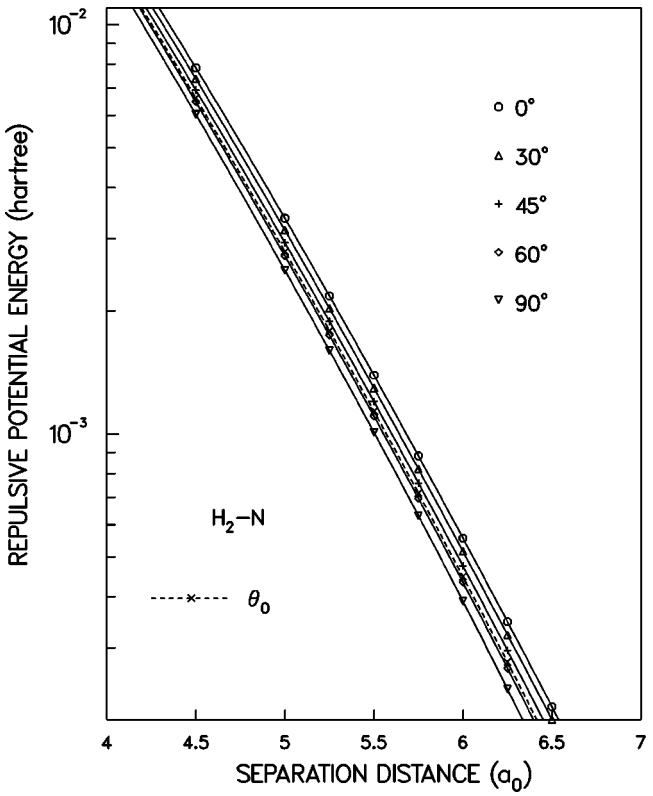

FIG. 3. H_2-N repulsive potential-energy curves at small r. The data points are obtained from the calculated results of the present work as described in the text; the curves are determined from spline fits to the data points. The curves obtained from $\overline{V}(r)$ and $V(r,\theta_0)$ are nearly indistinguishable as expected from the comparison of Fig. 1.

TABLE I. Expansion coefficients of the parameters (in atomic units) for $V_{MTT}(r,\theta)$.

	0	2	4
	H_2-N		
a	3.1348	−0.0074	
α	1.80776	−0.04409	0.00633
C_6	17.014 [a]	3.78 [b]	
C_8	314.9 [b]	177.2 [b]	
C_{10}	7761 [c]		
C_{12}	2.55×10^5 [c]		
	N_2-N		
a	5.0812	1.8661	−0.0197
α	1.85936	0.14671	−0.00578
C_6	41.96 [a]	5.41 [d]	
C_8	1117 [d]	849 [d]	
C_{10}	3.10×10^3 [c]		
C_{12}	8.97×10^5 [c]		

[a]Reference [30].
[b]Reference [31].
[c]Aufbau method of the Appendix.
[d]Determined from combination rules of Ref. [32] as described in the Appendix.

and are tabulated in Tables II and III for H_2-N and N_2-N, respectively. As shown in Table I, $a^{H_2\text{-}N}(\theta)$ has almost no angular variation; hence, according to Eq. (3b), the coefficient $F_2^{H_2\text{-}N}(r)$ of $P_2(\cos\theta)$ for $\ln[V_{SR}^{H_2\text{-}N}(r,\theta)]$ is nearly linear in r. On the other hand, $a^{N_2\text{-}N}(\theta)$ exhibits a much stronger angular variation compared to that of $a^{H_2\text{-}N}(\theta)$; in this case, the coefficient $F_2^{N_2\text{-}N}(r)$ has only a small radial variation at the intermediate values of r shown in Table III. At small r, $V(r,\theta)$ falls off more rapidly with decreasing r than a simple exponential function; a similar behavior was found [33] for N_2-N_2 interactions in the T configuration. As shown in Table III, this behavior is accompanied by a sharp rise in the number of P_{2n} required to describe $\ln[V_{SR}^c(r,\theta)]$ for small values of r.

The values of $V(r,\theta)$ that are obtained from the sum of $V_{SR}(r,\theta)$, determined using the coefficients of Table III, and $V_{DLR}(r,\theta)$, determined using Eq. (3c) and the coefficients of parameters listed in Table I, agree with our corresponding values of $V^c(r,\theta)$ to at least three significant figures when $V^c(r,\theta)$ is expressed in μE_h.

C. O_2-H and O_2-O interaction energies

The collisions involving a molecule of oxygen are more complex than those for nitrogen discussed above. Two states

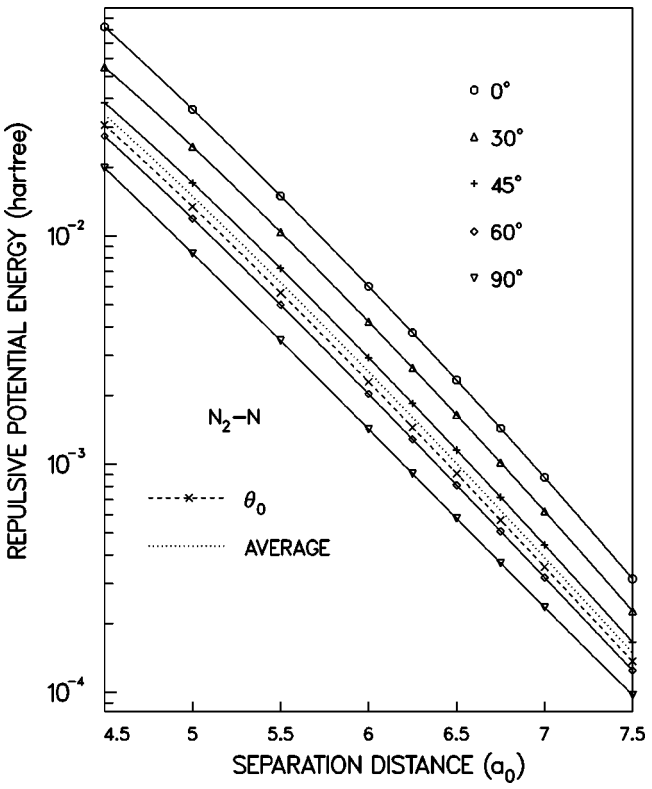

FIG. 4. N_2-N repulsive potential-energy curves at small r. The data points are obtained from the calculated results of the present work as described in the text; the curves are determined from spline fits to the data points.

of the HO_2 molecule are required to determine transport properties of the O_2-H interaction instead of a single state as in the above nitrogen interactions. Nine states are required to treat O_2-O collisions when the atom and molecule are in their ground states.

TABLE II. Expansion coefficients of $\ln[V_{SR}^c(r,\theta)]$ for H_2-N and V_{SR}^c in E_h.

r	$F_0^{H_2\text{-}H}(r)$	$F_2^{H_2\text{-}H}(r)$	$F_4^{H_2\text{-}H}(r)$
3.00	−2.7036	0.0331	0.0083
3.50	−3.4150	0.1017	−0.0024
4.00	−4.1925	0.1478	−0.0037
4.50	−5.0193	0.1767	−0.0054
5.00	−5.8847	0.1983	−0.0081
5.25	−6.3303	0.2083	−0.0097
5.50	−6.7844	0.2185	−0.0117
5.75	−7.2472	0.2297	−0.0147
6.00	−7.7193	0.2439	−0.0192
6.25	−8.2022	0.2635	−0.0258
6.50	−8.6988	0.2910	−0.0338
6.75	−9.2136	0.3282	−0.0427
7.00	−9.7540	0.3792	−0.0535
7.25	−10.3325	0.4569	−0.0717
7.50	−10.9770	0.6004	−0.1154

TABLE III. Expansion coefficients of $\ln[V_{SR}^c(r,\theta)]$ for N_2-N and V_{SR}^c in E_h.

r	$F_0^{N_2\text{-}N}(r)$	$F_2^{N_2\text{-}N}(r)$	$F_4^{N_2\text{-}N}(r)$	$F_6^{N_2\text{-}N}(r)$	$F_8^{N_2\text{-}N}(r)$
3.50	−2.1150	0.4971	0.3047	0.1801	0.1003
4.00	−2.7154	0.7959	0.1114	0.0575	0.0300
4.50	−3.4729	0.9197	0.0424	0.0105	0.0054
5.00	−4.3047	0.9626	0.0147	0.0004	
5.50	−5.1763	0.9733	0.0022		
6.00	−6.0755	0.9631	0.0011		
6.25	−6.5335	0.9499	0.0038		
6.50	−6.9960	0.9304	0.0087		
6.75	−7.4625	0.9036	0.0157		
7.00	−7.9320	0.8682	0.0249		
7.50	−8.8753	0.7640	0.0497		
8.00	−9.8108	0.5972	0.0804		

The O_2-H potential energy surfaces have been determined [29] using multireference configuration-interaction (MRCI) calculations with AQZ orbitals [24–26] and a multireference analog of the Davidson correction [34,35] to estimate the effect of higher excitations. A more detailed description of the computational methods can be found in Ref. [29].

A similar calculation is performed to determine the O_2-O interaction energies. For each spin, a state averaged complete-active-space self-consistent field (CASSCF) calculation with the oxygen $2p$ orbitals active is performed for the three spin states. The full CASSCF wave function is used for the reference space in the internally contracted CI where the core contains the $1s$ orbitals. An AQZ basis set [24–26] is used. At large r, the spin-orbit interaction is important; the energies of the coupled angular momentum states required for low-E scattering calculations might be obtained from the energies of the present approach by adapting a transformation [36,37] derived for atom-atom interactions. In this work, however, we focus on the transport properties at the higher temperatures where the spin-orbit interaction can be neglected. The spin-orbit contribution to transport properties at low temperatures is discussed in Ref. [38].

The calculated results at large r are shown in Fig. 5 for the orientation described by θ_0. The calculated result for $V_t(r)$, defined to be the average of the $V^n(r,\theta_0)$ for each state n of O_3 when weighted by the state degeneracy factor g_n, is also shown in Fig. 5. Note that the $V^n(r,\theta_0)$ for eight of the states are repulsive with weak van der Waals binding at large r; hence, the value of $V_t(r)$ is determined primarily by the high-spin repulsive states.

The contribution from a repulsive state to the transport properties is expected to be determined reasonably well from the effective potential represented by $V(r,\theta_0)$. The interaction energy for the lowest-lying singlet-spin state is large and the molecular complex is strongly bound; however, since the cross section for this state is weighted by only $1/27 \approx 0.037$, the error introduced in transport data from representing this state by $V(r,\theta_0)$ is considered to be insignificant.

D. Effective potential energies

We now determine an effective potential energy $V_e^{O_2\text{-}O}(r)$ that yields transport cross sections for O_2-O interactions for

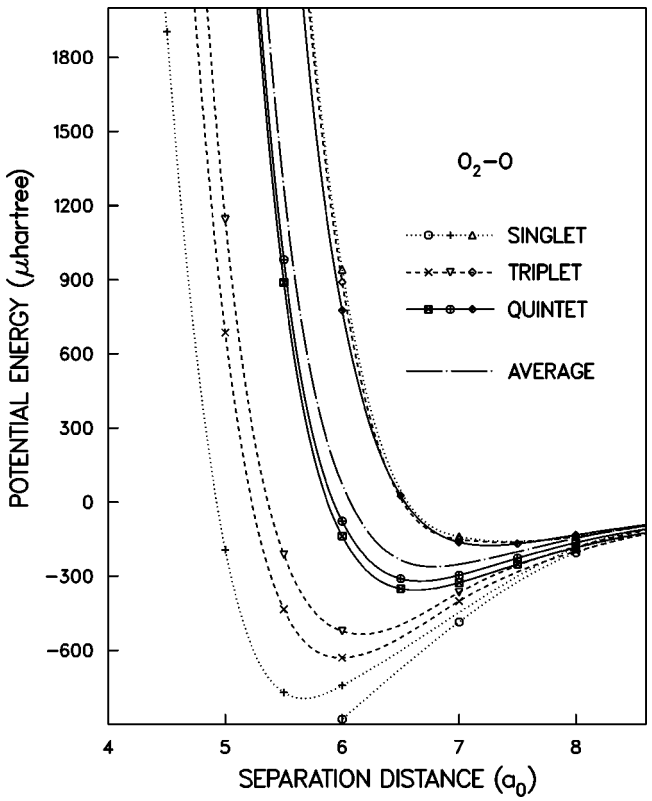

FIG. 5. O_2-O potential-energy curves at large r. The data points represent the calculated results of the present work for the angle θ_0. The dotted, dashed, and solid curves identify the O_2-O molecular states with spin $S=1/2$, 3/2, and 5/2, respectively. The dash-dotted curve is obtained from $V_t(r)$ as described in the text.

comparison with the $V_e(r)$ obtained by previous work. From the form [15] of the phase shifts η_l for large values of the quantum number l, one expects that $V_t(r)$ would be a reasonable choice for $V_e(r)$ at small values of E. From the form of collision integrals derived by Monchick [39] for an exponential potential, one expects [40] that $V_s(r)$, obtained from the degeneracy-weighted average of $\ln[V^c(r,\theta_0)]$ as described above, yields a better choice for $V_e(r)$ at small r when the repulsive potential parameters of $V(r)$ for the dominant repulsive states have about the same values. A more accurate determination of $V_e(r)$ follows from the treatment of multiple repulsive interactions in Ref. [40], but it is not considered necessary for this work. From the results of the present work described in the following section, we find that a suitable choice for $V_e^{O_2\text{-}O}(r)$ consists of $V_s(r)$ and $V_t(r)$ when r is smaller or larger, respectively, than about $5a_0$.

The two parameters σ [separation distance for which $V(\sigma)=0$] and the well depth ϵ, which are required for practical applications using a universal formulation [15] for transport properties, are determined from $V_e(r)$ and are listed in Table IV. The values of the parameters were determined from $V(r,\theta_0)$ for H_2-N and N_2-N interactions and from $V_t(r)$ for the O_2-O interaction. Our theoretical values are also compared with results that have been derived from measured data in Table IV. The theoretical and experimental results agree fairly well for N_2-N interactions. The experimental values for O_2-O interactions are not, however, reliable. As pointed out in Sec. I, the fit of the interaction energy of Ref. [11] to the diffusion measurements is not unique; furthermore, the above two potential parameters could not be determined uniquely in Ref. [42] since no structure (oscillatory behavior) was observed in the measured scattering cross section.

TABLE IV. Parameters for $V_e(r)$.

Interaction	σ (Å)	ϵ/κ (K)
	Theory	
H_2-N	3.017	56.9
N_2-N	3.349	90.1
O_2-O	3.205	80.7
	Experiment	
N_2-N	3.31 [a]	78 [a]
O_2-O	2.88 [a]	154 [a]
N_2-N	3.33 [b]	102 [b]
O_2-O	3.38 [c]	107 [c]

[a]Reference [11].
[b]Reference [41].
[c]Reference [42].

The $V_e(r)$ at small r of the present calculations are compared with some previous results that have been derived from measured data in Figs. 6 and 7 for N_2-N and O_2-O, respectively. The Lennard-Jones potential energies obtained [11] from diffusion measurements at room temperature agree fairly well with the present results at intermediate r, but predict too much repulsion at small r (which is characteristic of the short-range form of the chosen potential-energy function). The potential energies deduced from high-energy scattering measurements have a weaker repulsion than those of the present calculations at smaller r. The values of the exponential potential of Riabov [2] are slightly larger and close to the corresponding results of of Cubley and Mason [14] for N_2-N and O_2-O, respectively. The large uncertainty in the transport coefficients determined from scattering interaction energies is illustrated by the comparison of the results of Belyaev and Leonas [12] with those of Leonas [13] shown in Fig. 7.

The comparisons of the interaction energies shown in Figs. 6 and 7 indicate that the transport coefficients of Refs. [2] and [3] for N_2-N and of Ref. [3] for O_2-O are too large at high temperatures.

III. TRANSPORT COLLISION INTEGRALS AND PROPERTIES

Scattering calculations

The scattering cross section is calculated using the sudden approximation of Parker and Pack [43], which was derived using both centrifugal and energy sudden approximations. We have shown that this sudden approximation [43] yields H-H_2 collision integrals that are accurate [19]; i.e., our calculated values of the diffusion and viscosity coefficients agree with the corresponding results from close-coupling cal-

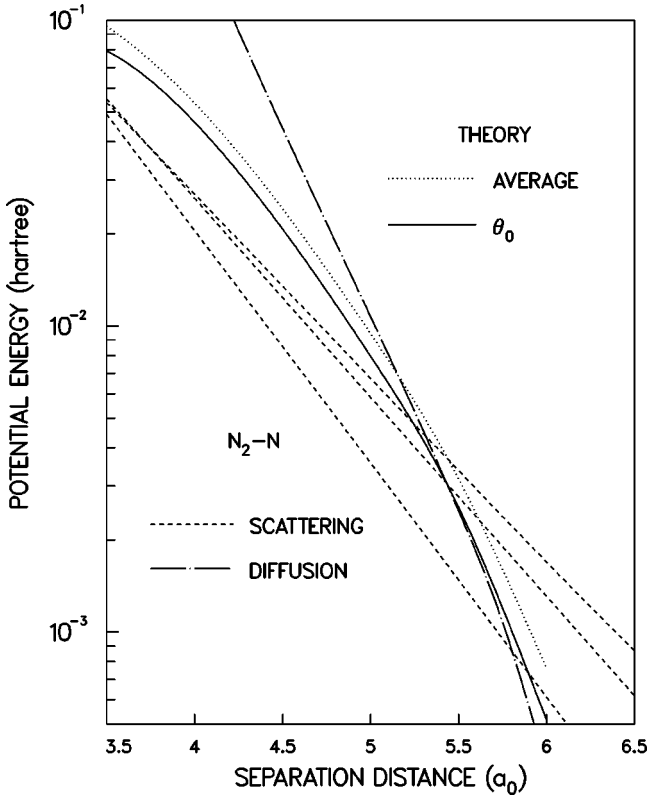

FIG. 6. Effective potential energies for the interaction of an atom and molecule of nitrogen at small r. The solid and dotted curves represent $V(r,\theta_0)$ and $\overline{V}(r)$, respectively. The dot-dashed curve is obtained from the interaction energy of Ref. [11]. The lower, intermediate, and upper dashed curves are obtained from the interaction energies of Refs. [13], [14], and [2], respectively.

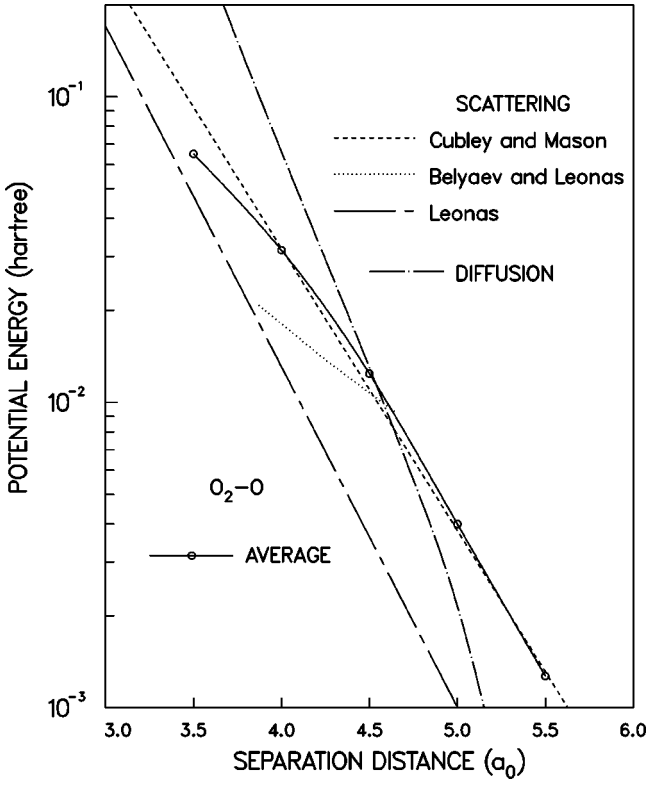

FIG. 7. Effective potential energies for the interaction of an atom and molecule of oxygen at small r. The solid curve is determined from $V_s(r)$. The dot-dashed, dotted, dashed, and long-short-dashed curves are obtained from the interaction energies of Refs. [11], [12], [14], and [13], respectively.

culations to within 1%. The theoretical diffusion agrees well [15,18,19] with the corresponding measurements for unlike collision partners. Similarly, the theoretical viscosity agrees well with the measurements for H_2-H_2 [19,44] and N_2-N_2 [15].

A quantum mechanical description is used to determine the scattering in the central field $V(r,\theta)$ for the orientation specified by θ. The values of the phase shift $\eta_l(E,\theta)$ for this orientation are calculated at lower E from a numerical integration of the Schrödinger equation, using the method presented by Levin *et al.* [45]. A semiclassical method [46] is used to determine $\eta_l(E,\theta)$ at E above a threshold energy E_t where the difference in the cross sections between the two methods does not exceed 0.3%.

The transport cross sections $Q_n(E,\theta)$ for each orientation are determined from the phase shifts by the sum

$$Q_n(E,\theta)=\frac{4\pi}{k^2}\sum_{l=0}^{\infty}\sum_{\nu>0}^{n} a_{n\nu}^{l}\sin^2[\,\eta_{l+\nu}(E,\theta)-\eta_l(E,\theta)\,] \tag{5}$$

where k is the wave number, and the allowed values of ν are even or odd according to the parity of n. The coefficients $a_{n\nu}^{l}$ can be determined from recursion relations [47].

For single-state interactions, the cross sections $\overline{Q}_n(E)$ that would be observed in the laboratory are obtained from an integral [18] of $Q_n(E,\theta)$ over all orientations. Multiple-state interactions require an additional calculation; $\overline{Q}_n(E)$ is obtained from the average of the cross section for each state weighted by the g factors. For O_2-H, the cross section for each state is determined separately from an integration over all orientations, but for O_2-O, as mentioned above, the cross sections for each state are determined from the $V(r,\theta_0)$ for that state. The collision integrals are determined from an average [48] over a Maxwell-Boltzmann velocity distribution; i.e.,

$$\Omega_{n,s}(T)=\frac{F(n,s)}{2(\kappa T)^{s+2}}\int_0^{\infty} e^{-E/\kappa T}E^{s+1}\overline{Q}_n(E)\,dE \tag{6}$$

where κ is the Boltzmann constant and $F(n,s)$ is a hard-sphere factor [47].

The calculated values of $\Omega_{n,s}(T)$ are listed in Tables V–VIII; the tabulated quantities allow the transport properties of a mixture to be determined to second order [48].

The calculated values of the interaction viscosity integral $\Omega_{2,2}(T)$ are compared with the corresponding values calculated from two candidates for an effective potential energy in Fig. 8 for H_2-N and N_2-N. Note that when the anisotropy is small, as for H_2-N interactions, the results obtained from

TABLE V. H_2-N collision integrals (Å^2).

T (K)	$\Omega_{1,1}$	$\Omega_{1,2}$	$\Omega_{1,3}$	$\Omega_{1,4}$	$\Omega_{1,5}$	$\Omega_{2,2}$	$\Omega_{2,3}$	$\Omega_{2,4}$	$\Omega_{3,3}$
100	9.61	8.40	7.79	7.41	7.12	10.61	9.66	9.11	9.04
150	8.38	7.54	7.08	6.75	6.49	9.34	8.70	8.29	8.11
200	7.73	7.04	6.62	6.33	6.09	8.68	8.16	7.81	7.58
300	6.97	6.42	6.05	5.77	5.55	7.94	7.52	7.21	6.95
400	6.51	6.00	5.66	5.42	5.21	7.46	7.09	6.84	6.54
600	5.93	5.47	5.19	4.89	4.65	6.90	6.57	6.27	6.02
800	5.54	5.09	4.73	4.52	4.35	6.49	6.10	5.89	5.57
1000	5.24	4.81	4.50	4.25	4.05	6.20	5.87	5.61	5.34
1500	4.72	4.31	4.00	3.75	3.54	5.66	5.33	5.06	4.82
2000	4.37	3.95	3.64	3.40	3.20	5.28	4.95	4.69	4.45
3000	3.87	3.46	3.16	2.92	2.72	4.75	4.42	4.16	3.95
4000	3.52	3.11	2.82	2.59	2.41	4.36	4.04	3.79	3.59
6000	3.03	2.64	2.36	2.14	1.94	3.84	3.53	3.25	3.11
8000	2.70	2.32	2.04	1.83	1.66	3.46	3.12	2.86	2.75
10000	2.45	2.08	1.81	1.61	1.44	3.16	2.83	2.57	2.48

$V(r,\theta_0)$ and $\overline{V}(r)$ are nearly the same. On the other hand, for N_2-N interactions with large anisotropy, the result for $\overline{V}(r)$ is slightly larger than that for $V(r,\theta_0)$. Past studies have usually used $\overline{V}(r)$ to construct $V_e(r)$ from measured data; however, the values of $V_e(r)$ taken from $V(r,\theta_0)$ are preferable since they provide a more accurate approximation to the transport properties and also require less computational effort.

The calculated values of $\Omega_{2,2}(T)$ are shown in Fig. 9 for O_2-H and O_2-O interactions. The value of $\Omega_{2,2}(T)$ for O_2-H is also determined from the $V(r,\theta_0)$ that are calculated [29] for each of the two required scattering states and shown in Fig. 9. This result is expected to be less accurate than that for O_2-O collisions since the value of g for the strongly bound ground state of O_2-H is about an order of magnitude larger than that for O_2-O discussed above. Note that the $V_e(r)$ from θ_0, however, provides a fairly good approximation to $\Omega_{2,2}$ as shown in Fig. 9 and requires a relatively small computational effort. Further note that the values of $\Omega_{2,2}$ for O_2-O agree well with the corresponding values determined from $V_e^{O_2\text{-}O}(r)$.

To focus on the physics of the interaction, we examine the reduced binary diffusion coefficient [44,49] defined by

$$D^*(T) = 10^4 T^{-3/2} (2\mu)^{1/2} D(T) \tag{7}$$

where μ is the reduced mass. Values of $D^*(T)$ are shown in Figs. 10 and 11 for N_2-N and O_2-O, respectively; the calculated values compare reasonably well with the corresponding results obtained from room temperature experiments. In particular, we show the results of Ref. [11], which are considered [52] to be the most reliable. Similar to the result found

TABLE VI. N_2-N collision integrals (Å^2).

T (K)	$\Omega_{1,1}$	$\Omega_{1,2}$	$\Omega_{1,3}$	$\Omega_{1,4}$	$\Omega_{1,5}$	$\Omega_{2,2}$	$\Omega_{2,3}$	$\Omega_{2,4}$	$\Omega_{3,3}$
100	15.04	12.70	11.45	10.70	10.16	16.56	14.65	13.43	13.76
150	12.65	11.02	10.17	9.63	9.24	13.94	12.59	11.77	11.86
200	11.41	10.15	9.47	9.04	8.72	12.58	11.57	10.95	10.87
300	10.10	9.20	8.69	8.31	8.04	11.21	10.52	10.05	9.85
400	9.39	8.63	8.18	7.89	7.64	10.47	9.92	9.57	9.26
600	8.57	7.96	7.58	7.25	6.98	9.68	9.23	8.88	8.58
800	8.08	7.50	7.08	6.83	6.68	9.17	8.70	8.45	8.04
1000	7.70	7.17	6.80	6.52	6.28	8.81	8.42	8.13	7.79
1500	7.07	6.58	6.22	5.93	5.69	8.19	7.81	7.51	7.19
2000	6.65	6.16	5.80	5.52	5.28	7.76	7.38	7.09	6.76
3000	6.06	5.59	5.22	4.93	4.68	7.16	6.79	6.50	6.18
4000	5.65	5.15	4.79	4.51	4.26	6.73	6.39	6.13	5.74
6000	5.05	4.56	4.17	3.83	3.50	6.18	5.82	5.50	5.14
8000	4.61	4.09	3.67	3.32	3.05	5.74	5.33	4.98	4.67
10000	4.25	3.71	3.28	3.02	2.73	5.36	4.92	4.54	4.31

TABLE VII. O_2-H collision integrals (Å^2).

T (K)	$\Omega_{1,1}$	$\Omega_{1,2}$	$\Omega_{1,3}$	$\Omega_{1,4}$	$\Omega_{1,5}$	$\Omega_{2,2}$	$\Omega_{2,3}$	$\Omega_{2,4}$	$\Omega_{3,3}$
100	9.79	8.65	8.03	7.62	7.30	10.84	9.98	9.44	9.34
150	8.60	7.76	7.25	6.88	6.60	9.64	8.99	8.55	8.38
200	7.93	7.20	6.75	6.43	6.18	8.95	8.41	8.03	7.81
300	7.12	6.53	6.14	5.85	5.59	8.16	7.71	7.38	7.12
400	6.63	6.08	5.70	5.44	5.21	7.66	7.25	6.96	6.67
600	6.04	5.50	5.17	4.91	4.70	7.04	6.68	6.39	6.11
800	5.58	5.12	4.81	4.60	4.45	6.61	6.25	6.02	5.73
1000	5.27	4.88	4.58	4.37	4.18	6.32	5.99	5.74	5.48
1500	4.81	4.41	4.11	3.85	3.63	5.78	5.44	5.15	4.97
2000	4.45	4.05	3.74	3.48	3.27	5.38	5.02	4.72	4.57
3000	3.96	3.54	3.22	2.97	2.76	4.80	4.44	4.16	4.02
4000	3.59	3.17	2.86	2.63	2.44	4.38	4.04	3.78	3.63
6000	3.09	2.69	2.38	2.15	1.94	3.84	3.50	3.23	3.13
8000	2.74	2.34	2.05	1.82	1.65	3.45	3.10	2.83	2.74
10000	2.47	2.08	1.80	1.60	1.43	3.14	2.80	2.54	2.47

for the viscosity in Fig. 8, we find that $V(r,\theta_0)$ is a good $V_e(r)$ for determining the diffusion for the interactions with N_2. Consistent with the comparisons of Figs. 7 and 11, one finds that our present calculations indicate that the exponential potential energy of Ref. [14] provides a suitable $V_e(r)$ for predicting the O_2-O transport properties for a wide range of high temperatures.

IV. SUMMARY AND CONCLUSIONS

The potential-energy surfaces for the interactions of a nitrogen atom with the diatomic molecules of nitrogen and hydrogen are calculated using high-level quantum chemistry methods. The transport collision integrals have been calculated from these interactions and used to confirm that an effective potential energy determined from the θ_0 orientation yields accurate transport data with a small computational effort; the θ_0 orientation is especially important for collisions with large molecular anisotropy. Our calculated N_2-N and O_2-O diffusion coefficients agree well with the corresponding measurements from low-temperature experiments, but we find that our high-temperature transport coefficients are considerably smaller than some estimates that were recommended for aerospace studies prior to our work.

An Aufbau method for determining the dispersion coefficients of effective potential energies from the data for other interactions is developed and applied to obtain higher-order coefficients for the atom-molecule interactions of hydrogen and nitrogen.

Transport data for O_2-H are calculated and compared with the prediction obtained from the θ_0 orientation. The O_2-O interaction energies are calculated for the θ_0 orientation of all the O_3 states required for collision studies and applied to determine transport data. Our results agree well with both the

TABLE VIII. O_2-O collision integrals (Å^2).

T (K)	$\Omega_{1,1}$	$\Omega_{1,2}$	$\Omega_{1,3}$	$\Omega_{1,4}$	$\Omega_{1,5}$	$\Omega_{2,2}$	$\Omega_{2,3}$	$\Omega_{2,4}$	$\Omega_{3,3}$
100	13.68	11.81	10.55	9.67	9.12	15.31	13.58	12.30	12.71
150	11.58	9.98	9.15	8.59	8.24	12.70	11.51	10.68	10.79
200	10.32	9.15	8.46	8.04	7.73	11.49	10.49	9.87	9.84
300	9.10	8.20	7.69	7.33	7.07	10.13	9.43	8.96	8.82
400	8.39	7.64	7.21	6.91	6.67	9.39	8.83	8.49	8.23
600	7.58	6.99	6.66	6.30	6.05	8.61	8.18	7.87	7.66
800	7.09	6.55	6.15	5.87	5.62	8.13	7.71	7.42	7.09
1000	6.74	6.21	5.84	5.55	5.31	7.78	7.39	7.09	6.78
1500	6.11	5.62	5.27	5.00	4.78	7.15	6.77	6.46	6.20
2000	5.70	5.23	4.89	4.64	4.45	6.71	6.33	6.02	5.80
3000	5.15	4.71	4.40	4.16	3.97	6.09	5.72	5.43	5.25
4000	4.78	4.36	4.07	3.85	3.68	5.67	5.32	5.07	4.87
6000	4.29	3.90	3.64	3.41	3.22	5.13	4.86	4.58	4.39
8000	3.96	3.61	3.32	3.10	2.92	4.78	4.45	4.23	4.03
10000	3.71	3.35	3.08	2.87	2.70	4.50	4.20	3.95	3.79

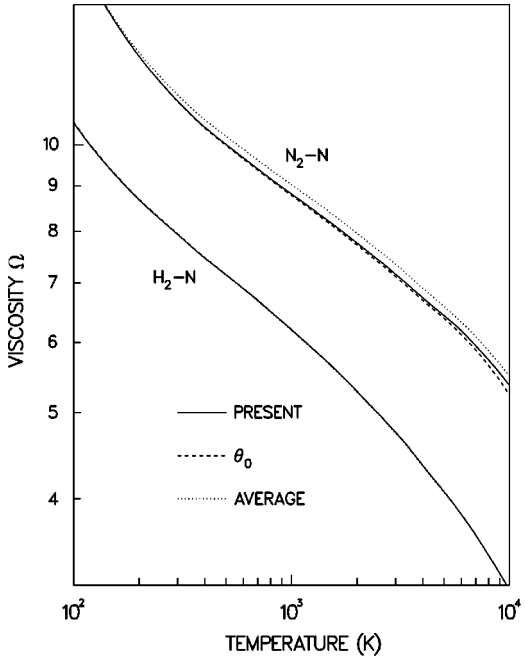

FIG. 8. The values of $\Omega_{2,2}(T)$ in units of Å as a function of temperature in K for collisions of the molecules of hydrogen and oxygen with oxygen atoms. The solid curves are obtained from Tables V and VI. The dashed and dotted curves are determined from $V(r,\theta_0)$ and $\overline{V}(r)$, respectively; for H_2-N, these curves are nearly hidden by the solid curve.

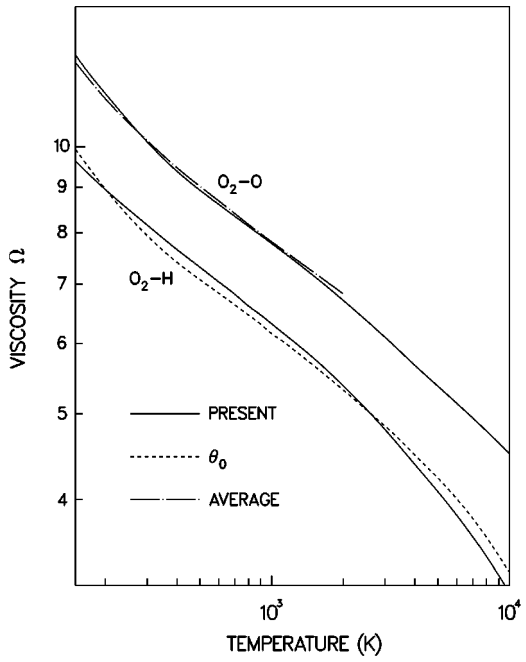

FIG. 9. The values of $\Omega_{2,2}(T)$ in units of Å as a function of temperature in K for collisions of the molecules of oxygen with hydrogen or nitrogen atoms. The solid curves are obtained from Tables VII and VIII. The dashed curve is determined from $V(r,\theta_0)$ for O_2-H and the dot-dashed curve is determined from the $V_e^{O_2\text{-}O}(r)$ described in the text.

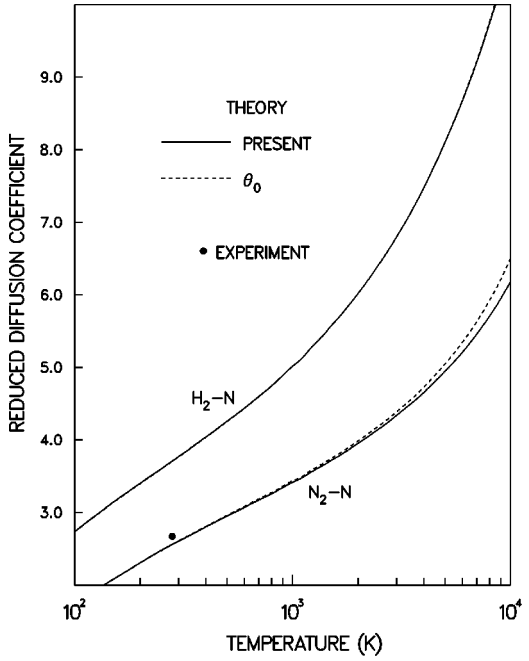

FIG. 10. The value of $pD^*(T)$ as a function of temperature in K for the collisions of molecules of hydrogen and nitrogen with nitrogen atoms at a pressure of 1 atm. The dashed curve is obtained from $V(r,\theta_0)$; for H_2-N, this curve is nearly hidden by the solid curve. The data point is obtained from the diffusion measurements of Ref. [11] for N_2-N.

low-temperature diffusion measurements and the transport data determined from the potential energies deduced from high-energy scattering measurements. Furthermore, our results indicate that the effective potential energies determined from the θ_0 orientation yield accurate transport data for multiple-state collisions when the scattering is dominated by the repulsive states.

ACKNOWLEDGMENT

Support for E.L. was provided by Contract No. NAS2-99092 from NASA to the Eloret Corporation.

APPENDIX: AUFBAU DISPERSION COEFFICIENTS

The spherically averaged long-range coefficients $\overline{C}_{2n}$ are sufficient for determining the long-range force for $V_e(r)$ specified by the θ_0 orientation for atom-molecule collisions or the dd' [15] orientation (the polar angles are specified by θ_0 and the azimuthal angle is $\pi/2$) for molecule-molecule interactions. Fortunately, the scattering calculations described above do not require highly accurate values for these coefficients. Likewise, approximate values of C_{2n} are sufficient for determining the short-range interaction for $V_e(r)$; i.e., using Eq. (4) for atom-molecule interactions or the corresponding relation [15] for molecule-molecule interactions. In general, the calculation of the coefficients requires a large computational effort. We outline an Aufbau procedure that may allow the $\overline{C}_{2n}$ to be readily estimated from an incomplete data base for the coefficients; e.g., when the higher-

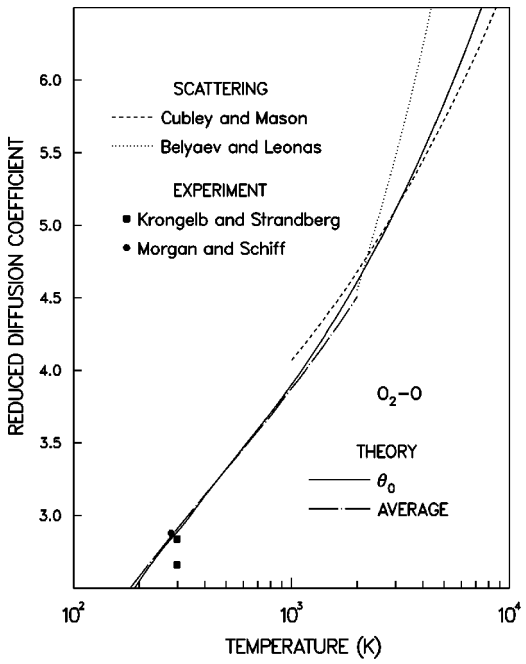

FIG. 11. The value of $pD^*(T)$ as a function of temperature in K for the collisions of molecules of oxygen with oxygen atoms at a pressure of 1 atm. The solid curve is calculated from the values of $V(r,\theta_0)$ for all the states of the O_2-O molecule. The dot-dashed curve is obtained from the $V_e^{O_2\text{-}O}(r)$ described in the text. The dashed curve is calculated from the interaction energy of Ref. [14]; the dotted curve is obtained from tabulation of Ref. [50]. The data points are obtained from the diffusion measurements of Refs. [11] and [51].

order C_{2n} for atom-atom and molecule-molecule interactions are known, but values for the atom–molecule C_{2n} are not available. We determine values for the atom-molecule C_{2n} needed for the hydrogen-nitrogen interactions of the present work.

Kramer and Herschbach [53] have derived combining relations that allow the values of C_{2n} for unlike interactions to be determined from the values for like interactions. Defining a reduced coefficient

$$c_{2n}^{a\text{-}b}=\frac{C_{2n}^{a\text{-}b}}{\alpha^a\alpha^b}, \tag{A1}$$

where α is the dipole polarizability, their combining relation for $n=3$ has the simple form

$$\frac{1}{c_6^{a\text{-}b}}=\frac{1}{2}\left(\frac{1}{c_6^{a\text{-}a}}+\frac{1}{c_6^{b\text{-}b}}\right). \tag{A2}$$

The rms error in the C_6 obtained from Eq. (A2) was examined [54] for over 200 interactions and found to be only about 0.5%. For $n=4$, their combining relation [53] can be written as

$$c_8^{a\text{-}b}=\frac{1}{2}\left(\frac{c_8^{a\text{-}a}}{1-\delta_6^{a,b}\zeta^a c_8^{a\text{-}a}}+\frac{c_8^{b-b}}{1+\delta_6^{a,b}\zeta^b c_8^{b-b}}\right) \tag{A3a}$$

where we have defined the quantities

$$\delta_6^{a,b}=\frac{1}{2}\left(\frac{1}{c_6^{a\text{-}a}}-\frac{1}{c_6^{b\text{-}b}}\right), \tag{A3b}$$

$$\zeta^a=\frac{1}{5}\frac{\alpha^a}{q^a}, \tag{A3c}$$

$$\zeta^b=\frac{1}{5}\frac{\alpha^b}{q^b}, \tag{A3d}$$

and q is the quadrupole polarizability.

If $c_6^{a\text{-}a}\approx c_6^{b\text{-}b}$, then Eq. (A3) reduces to the simple relation

$$c_8^{a\text{-}b}=\frac{1}{2}(c_8^{a\text{-}a}+c_8^{b\text{-}b}). \tag{A4}$$

Furthermore, the average of the quantities on the RHS of Eq. (A2) can be replaced by the geometric mean of the corresponding quantities and Eq. (A2) yields a rigorous upper bound [55,56] to $C_6^{a\text{-}b}$. In addition, if $c_8^{a\text{-}a}\approx c_8^{b\text{-}b}$, then the dispersion coefficients for both $n=3$ and 4 are approximately related by expressions of the form

$$C_{2n}^{b\text{-}b}\approx P_{2n}^{a\text{-}b}C_{2n}^{a\text{-}b}\approx(P_{2n}^{a\text{-}b})^2C_{2n}^{a\text{-}a} \tag{A5}$$

where the Aufbau factors (to lowest order) are

$$P_{2n}^{a\text{-}b}\approx\frac{\alpha^b}{\alpha^a}. \tag{A6}$$

When the c_{2n} for a family of interaction systems have about the same value, e.g.,

$$c_{2n}^{a\text{-}a}\approx c_{2n}^{b\text{-}b}\approx c_{2n}^{c\text{-}c}, \tag{A7}$$

the Aufbau factors are related by

$$P_{2n}^{a\text{-}c}=P_{2n}^{a\text{-}b}P_{2n}^{b\text{-}c}. \tag{A8}$$

Mulder *et al.* [57] have found a number of combining relations [Eqs. (34) of Ref. [57]] that are useful for obtaining approximate values of C_{2n} for various molecular interactions. For example, their relations specify that both $C_6^{a\text{-}b}$ and $C_{10}^{a\text{-}b}$ for unlike interactions are obtained from the geometric mean of the coefficients for the like interactions as described above. Using relations (A5) and (A6) for $n=5$, one obtains relation (A4) from their combining relation for C_8. Furthermore, relations (A5) for $n=5$ can be obtained from the approximation (Sec. III B of Ref. [58] to P_{10}) developed by Thakkar [58] when the C_{2n} for $n\leqslant 4$ satisfy relations (A5). Hence, we assume that relations (A5) are valid also for $n=5$ when they hold for $n=3$ and 4.

We find that the Aufbau relations (A5) and (A8) provide an excellent correlation of the accurate C_{2n} for the family of interactions formed from hydrogen and rare-gas atoms. In the following application, we examine the correlation of the known C_{2n} of the family of interactions formed from the atoms and molecules of hydrogen and nitrogen and determine the atom-molecule C_{2n} for the three interactions with

TABLE IX. Aufbau factors for the interaction of hydrogen and nitrogen.

n	$P_{2n}^{\text{H-N}}$	$P_{2n}^{\text{H-H}_2}$	$P_{2n}^{\text{H}_2\text{-N}_2}$
3	1.91	1.36	2.45
4	1.92	1.31	3.46
5	1.92	1.22	4.04

the largest masses. For convenience of applications, note from Eqs. (A5) that the Aufbau factors can be considered to be exchange operators, e.g., the effect of multiplying by the factor $P_{2n}^{a\text{-}b}$ is to change particle a into particle b. Note further from Eq. (A8) that the values of C_{2n} for all members of the hydrogen-nitrogen family can be obtained from the values of $C_{2n}^{\text{H-H}}$, which have been calculated [58] very accurately, when a few values of the Aufbau factors are known. For example, from relations (A5) and (A8), the N-N_2 atom-molecule dispersion coefficient can be approximated from the construction

$$C_{2n}^{\text{N-N}_2} = P_{2n}^{\text{H}_2\text{-N}_2} P_{2n}^{\text{H-H}_2} P_{2n}^{\text{H-N}} C_{2n}^{\text{H}-\text{H}}. \tag{A9}$$

The required values of P_{2n} can be extracted from a limited C_{2n} data base using Eqs. (A5); however, we find that the accuracy of the C_{2n} obtained from the Aufbau method is improved by increased size and quality of the data base.

The values of $P_{2n}^{a\text{-}b}$ for the unlike interactions appearing on the RHS of Eq. (A9) are determined from the C_{2n} data available for H_2-H interactions and from the atom-atom and molecule-molecule interactions of hydrogen and nitrogen; the results are listed in Table IX. The values of $C_{2n}^{\text{H}_2\text{-H}}$ have been calculated accurately by Bishop and Pippin [59] and by Meyer, reported in Ref. [60]. Accurate values of C_6 for all 10 interactions of the hydrogen-nitrogen family have been determined from measured data by Meath and co-workers [30,61,62]. The data for the higher-order C_{2n} of the other interactions are less accurate than those described above because of uncertainties introduced by the methods of calculation. The C_{2n} of atom-atom interactions are taken from Table V of Ref. [63]. The C_{2n} for molecule-molecule interactions have been calculated for H_2-H_2 [64,65], N_2-H_2 [66,67], and N_2-N_2 [66,67]. The values of P_{2n} listed in Table IX for atom-atom and molecule-molecule interactions are the average of the two values obtained using Eqs. (A5).

We find that the values of Table IX provide an adequate correlation of the atom-atom and molecule-molecule data and predict the atom-molecule C_{2n} fairly well. For example, the rms error in C_6 obtained from $C_6^{\text{H-H}}$, using the Aufbau factors of Table IX and the building-up relations illustrated by Eq. (A9), for the other nine members of the hydrogen-nitrogen family is only about 1%. The value of $C_8^{\text{H}_2\text{-N}}$ obtained using the Aufbau method described above is less than 1% smaller than the value of $\overline{C}_8$ calculated by Hettema and Wormer [31] using a time-dependent coupled Hartree-Fock method.

We have determined the values of the coefficients of the atom-molecule $C_{2n}(\theta)$ for an expansion in $P_{2n}(\cos\theta)$ when $n=3$ and 4 from the combining relations of Fuchs *et al.* [32], using the atom-atom and molecule-molecule data described above. The molecule-molecule values tabulated for C_{2n} in the space-fixed frame are transformed to the body-fixed frame using the formulation of Ref. [66]. Our results are contained in Table I; the values obtained for $\overline{C}_8^{\text{N}_2\text{-H}}$ and $\overline{C}_8^{\text{N}_2\text{-N}}$ are about the same and 3% larger, respectively, than the corresponding values obtained from the Aufbau method. The determination of C_8 from the combining relations of Ref. [32] is relatively difficult since the solution of five nonlinear equations is required; the above comparisons are useful for assessing the validity of the results obtained for C_8. Furthermore, the comparisons also indicate that the corrections from α and q (including the required components) to the Aufbau value of C_8 are small, i.e., their contribution to C_8 is nearly accounted for by the Aufbau method.

The values of atom-molecule C_{10} obtained from $C_{10}^{\text{H}-\text{H}}$ and the Aufbau factors of Table IX are listed in Table I. We are not aware of other values for comparison; however, the known data are correlated fairly well (i.e., the rms value for the differences between the Aufbau values of C_{10} obtained from $C_{10}^{\text{H-H}}$ and the data described above for the other two atom-atom and the three molecule-molecule interactions is about 2%).

Higher-order C_{2n} can be estimated from recursive relations [58,68]; e.g.,

$$C_{2n+4}^{a\text{-}b} = (C_{2n+2}^{a\text{-}b}/C_{2n}^{a\text{-}b})^3 C_{2n-2}^{a\text{-}b} \tag{A10}$$

for $n \geqslant 4$. When the lower-order C_{2n} satisfy relations (A5) the higher-order Aufbau factors can be obtained from

$$P_{2n+4}^{a\text{-}b} = (P_{2n+2}^{a\text{-}b}/P_{2n}^{a\text{-}b})^3 P_{2n-2}^{a\text{-}b}. \tag{A11}$$

Equation (A10) is used to obtain the values of $\overline{C}_{12}$ that are listed in Table I from the values of $\overline{C}_{2n}$ for $n \leqslant 5$.

[1] T. W. Megli, H. Krier, and R. L. Burton, J. Thermophys. Heat Transfer **10**, 554 (1996).

[2] V. V. Riabov, J. Thermophys. Heat Transfer **10**, 209 (1995).

[3] M. Capitelli, C. Gorse, S. Longo, and D. Giordano, J. Thermophys. Heat Transfer **14**, 259 (2000).

[4] C. Park, R. L. Jaffe, and H. Partridge, J. Thermophys. Heat Transfer **15**, 76 (2001).

[5] A. B. Murphy, Phys. Rev. E **48**, 3594 (1993).

[6] A. B. Murphy and C. J. Arundell, Plasma Chem. Plasma Process. **14**, 451 (1994).

[7] A. B. Murphy, Plasma Chem. Plasma Process. **15**, 279 (1995).

[8] A. D. Tserpi and T. A. Miller, J. Appl. Phys. **77**, 505 (1995).

[9] J. G. Cook, L. LeBrun, L. Zhongming, and E. A. Ogryzlo, J. Appl. Phys. **77**, 1690 (1995).

[10] J. V. Michael and K. P. Lim, J. Chem. Phys. **97**, 3228 (1992).
[11] J. E. Morgan and H. I. Schiff, Can. J. Chem. **42**, 2300 (1964).
[12] Yu. N. Belyaev and V. B. Leonas, Zh. Éksp. Teor. Fiz. Pis'ma Red. **4**, 134 (1966) [JETP Lett. **4**, 92 (1966)].
[13] V. B. Leonas, Usp. Fiz. Nauk **107**, 29 (1972) [Sov. Phys. Usp. **15**, 266 (1973)].
[14] S. J. Cubley and E. A. Mason, Phys. Fluids **18**, 1109 (1975).
[15] J. R. Stallcop, H. Partridge, and E. Levin, Phys. Rev. A **62**, 062709 (2000).
[16] *Computational Modeling in Semiconductor Processing*, edited by M. Meyyapan (Artech House, Boston, 1995).
[17] J. Bzowski, J. Kestin, E. A. Mason, and F. J. Uribe, J. Phys. Chem. Ref. Data **19**, 1179 (1990).
[18] J. R. Stallcop, H. Partridge, S. P. Walch, and E. Levin, J. Chem. Phys. **97**, 3431 (1992).
[19] J. R. Stallcop, H. Partridge, and E. Levin, Chem. Phys. Lett. **254**, 25 (1996).
[20] R. J. Bartlett, Annu. Rev. Phys. Chem. **32**, 359 (1981).
[21] P. J. Knowles, C. Hampel, and H.-J. Werner, J. Chem. Phys. **99**, 5219 (1993).
[22] K. Raghavachari, G. W. Trucks, J. A. Pople, and M. Head-Gordon, Chem. Phys. Lett. **157**, 479 (1989).
[23] J. D. Watts, J. Gauss, and R. J. Bartlett, J. Chem. Phys. **98**, 8718 (1993).
[24] T. H. Dunning, J. Chem. Phys. **90**, 1007 (1989).
[25] R. A. Kendall, T. H. Dunning, and R. J. Harrison, J. Chem. Phys. **96**, 6796 (1992).
[26] D. E. Woon, K. A. Peterson, and T. H. Dunning, J. Chem. Phys. **98**, 1358 (1993).
[27] S. F. Boys and F. Bernardi, Mol. Phys. **19**, 533 (1970).
[28] H. Partridge and C. W. Bauschlicher, Mol. Phys. **96**, 705 (1999).
[29] J. R. Stallcop, H. Partridge, and E. Levin, Phys. Rev. A **53**, 766 (1996).
[30] D. J. Margoliash and W. J. Meath, J. Chem. Phys. **68**, 1426 (1978).
[31] H. Hettema and P. E. S. Wormer, J. Chem. Phys. **93**, 3389 (1990).
[32] R. R. Fuchs, F. R. W. McCourt, A. J. Thakkar, and F. Grein, J. Phys. Chem. **88**, 2036 (1984).
[33] J. R. Stallcop and H. Partridge, Chem. Phys. Lett. **281**, 212 (1997).
[34] S. R. Langhoff and E. R. Davidson, Int. J. Quantum Chem. **8**, 61 (1974).
[35] M. R. A. Blomberg and P. E. M. Siegbahn, J. Chem. Phys. **78**, 5682 (1978).
[36] J. S. Cohen and B. Schneider, J. Chem. Phys. **61**, 3230 (1974).
[37] A. P. Hickman, M. Medikeri-Naphade, C. D. Chapin, and D. L. Heustis, Phys. Rev. A **56**, 4633 (1997).
[38] E. Levin, J. R. Stallcop, and H. Partridge, Theor. Chem. Acc. **103**, 518 (2000).
[39] L. Monchick, Phys. Fluids **2**, 695 (1959).
[40] H. Partridge, J. R. Stallcop, and E. Levin, J. Chem. Phys. (to be published).
[41] F. Pirani, D. Cappelletti, and V. Aquilanti, in *Molecular Physics and Hypersonic Flows*, edited by M. Capitelli (Kluwer Academic, Dordrecht, 1996), pp. 351–360.
[42] B. Brunetti, G. Liuti, E. Luzzatti, F. Pirani, and F. Vecchiocattivi, J. Chem. Phys. **74**, 6734 (1981).
[43] G. A. Parker and R. T. Pack, J. Chem. Phys. **68**, 1585 (1978).
[44] J. R. Stallcop, E. Levin, and H. Partridge, J. Thermophys. Heat Transfer **12**, 514 (1998).
[45] E. Levin, D. W. Schwenke, J. R. Stallcop, and H. Partridge, Chem. Phys. Lett. **227**, 669 (1994).
[46] J. R. Stallcop, H. Partridge, and E. Levin, J. Chem. Phys. **95**, 6429 (1991).
[47] E. Levin, H. Partridge, and J. R. Stallcop, J. Thermophys. Heat Transfer **4**, 469 (1990).
[48] G. C. Maitland, M. Rigby, E. B. Smith, and W. A. Wakeham, *Intermolecular Forces. Their Origin and Determination* (Oxford University Press, Oxford, 1981).
[49] J. O. Hirschfelder, C. F. Curtiss, and R. B. Bird, *Molecular Theory of Gases and Liquids* (Wiley-Interscience, New York, 1964).
[50] Yu. N. Belyaev and V. B. Leonas, Teplofiz. Vys. Temp. **6**, 188 (1968) [Sov. Phys. High Temp. **6**, 182 (1968)].
[51] S. Krongelb and M. W. P. Strandberg, J. Chem. Phys. **31**, 1196 (1959).
[52] T. R. Marrero and E. A. Mason, J. Phys. Chem. Ref. Data **1**, 3 (1972).
[53] H. L. Kramer and D. R. Herschbach, J. Chem. Phys. **53**, 2792 (1970).
[54] A J. Thakkar, J. Chem. Phys. **81**, 1919 (1984).
[55] K. T. Tang, J. Chem. Phys. **49**, 4727 (1968).
[56] F. Weinhold, J. Phys. B **2**, 517 (1969).
[57] F. Mulder, G. F. Thomas, and W. J. Meath, Mol. Phys. **41**, 249 (1980).
[58] A. J. Thakkar, J. Chem. Phys. **89**, 2092 (1988).
[59] D. M. Bishop and J. Pippin, J. Chem. Phys. **98**, 522 (1993).
[60] K. T. Tang and J. P. Toennies, Chem. Phys. Lett. **151**, 301 (1988).
[61] G. D. Zeiss and W. J. Meath, Mol. Phys. **33**, 1155 (1977).
[62] W. J. Meath and A. Kumar, Int. J. Quantum Chem., Symp. **24**, 501 (1990).
[63] J. R. Stallcop, C. W. Bauschlicher, H. Partridge, S. R. Langhoff, and E. Levin, J. Chem. Phys. **97**, 5578 (1992).
[64] F. Visser, P. E. S. Wormer, and W. P. J. H. Jacobs, J. Chem. Phys. **82**, 3753 (1985).
[65] J. Schaefer and W. E. Köhler, Z. Phys. D: At., Mol. Clusters **13**, 217 (1989).
[66] F. Visser, P. E. S. Wormer, and P. Stam, J. Chem. Phys. **79**, 4973 (1983).
[67] W. Rijks and P. E. S. Wormer, J. Chem. Phys. **88**, 5704 (1988).
[68] K. T. Tang and J. P. Toennies, J. Chem. Phys. **80**, 3726 (1984).